Color Image Restoration Using Nonlocal Mumford-Shah Regularizers

Miyoun Jung, Xavier Bresson, Tony F. Chan, and Luminita A. Vese

Department of Mathematics, University of California, Los Angeles, CA 90095, U.S.A.
{gomtaeng,xbresson,chan,lvese}@math.ucla.edu

Abstract. We introduce several color image restoration algorithms based on the Mumford-Shah model and nonlocal image information. The standard Ambrosio-Tortorelli and Shah models are defined to work in a small local neighborhood, which are sufficient to denoise smooth regions with sharp boundaries. However, textures are not local in nature and require semi-local/non-local information to be denoised efficiently. Inspired from recent work (NL-means of Buades, Coll, Morel and NL-TV of Gilboa, Osher), we extend the standard models of Ambrosio-Tortorelli and Shah approximations to Mumford-Shah functionals to work with nonlocal information, for better restoration of fine structures and textures. We present several applications of the proposed nonlocal MS regularizers in image processing such as color image denoising, color image deblurring in the presence of Gaussian or impulse noise, color image inpainting, and color image super-resolution. In the formulation of nonlocal variational models for the image deblurring with impulse noise, we propose an efficient preprocessing step for the computation of the weight function w. In all the applications, the proposed nonlocal regularizers produce superior results over the local ones, especially in image inpainting with large missing regions. Experimental results and comparisons between the proposed nonlocal methods and the local ones are shown.

1 Introduction

We consider the restoration problem of a color image formalized as

$$f = Hu + n, \quad (f^i = H^i u^i + n^i,\ i = r, g, b) \tag{1}$$

where H is a linear operator accounting for some blurring, sub-sampling or missing pixels so that the observed data $f : \Omega \to \mathbb{R}$ loses some portion of the original image u we wish to recover, and n is an additive noise. We approach the restoration problem within the variational framework: $\inf_u\{\Phi(f - Hu) + \Psi(|\nabla u|)\}$, where Φ defines a data-fidelity term, and Ψ defines the regularization that enforces a smoothness constraint on u, depending on its gradient ∇u.

Problem (1) is ill-posed, but the regularization term Ψ alleviates this difficulty by reflecting some a priori properties. Several edge-preserving regularization terms were suggested in the literature, including [9], [20], [2], [21], [5], [4]. These traditional regularization terms are based on local image operators, which

D. Cremers et al. (Eds.): EMMCVPR 2009, LNCS 5681, pp. 373–387, 2009.
© Springer-Verlag Berlin Heidelberg 2009

denoise and preserve edges and smooth regions very well, but may not deal well with fine structures like texture during the restoration process because textures are not local in nature.

Recently, new image denoising models have been developed, based on nonlocal image operators, to better deal with textures. Buades et al [8] introduced the nonlocal means filter, which produces excellent denoising results. Kindermann et al [13], and Gilboa-Osher [10,11] formulated the variational framework of NL-means by proposing nonlocal regularizing functionals. Lou et al [14] used the nonlocal total variation of Gilboa-Osher (NL/TV) in grey-scale image deblurring in the presence of Gaussian noise. Moreover, Peyré et al [18] used NL/TV for grey-scale image inpainting, super-resolution of a single image, and compressive sensing. Protter et al. [19] generalized the NL-means filter to super-resolution.

The previous works on nonlocal methods have been done on the Gaussian noise model, but no study has been developed on the impulse noise model using non-local information. However, the impulsive noise model was studied in the local case. Bar et al [4] used the Ambrosio-Tortorelli and Shah approximations to Mumford-Shah regularizing functional for color image deblurring in the presence of impulse noise, producing better restorations than total variation (TV) regularizer, and moreover providing the edge set detected concurrently with the restoration process. We propose in this paper the nonlocal versions of Ambrosio-Tortorelli [2] and Shah [21] approximations to the Mumford-Shah regularizer for the multichannel case. We also propose (a) several applications of the NL/MS for color image denoising, deblurring in the presence of Gaussian or impulse noise, inpainting with large missing portion, super-resolution of a single image, and (b) an efficient preprocessing step to compute the weights w in the deblurring-denoising model in the presence of impulse noise.

2 Background

Local regularizer. We recall two approximations of the Mumford-Shah-like regularizing functionals [16] that have been used in several algorithms. The MS regularizer, depending on the image u and on its edge set $K \subset \Omega$, gives preference to piecewise smooth images: $\Psi^{MS}(u, K) = \beta \int_{\Omega \setminus K} |\nabla u|^2 dx + \alpha \int_K d\mathcal{H}^1$, where $\mathcal{H}^1$ is the 1D Hausdorff measure. The first term enforces smoothness of u everywhere except on the edge set K, and the second one minimizes the total length of edges. It is difficult to minimize in practice the non-convex MS functional. One approach is using phase field by Γ-convergence with applications to image deblurring and denoising [3], and inpainting [22]. More specifically, Ambrosio-Tortorelli [2] approximated the MS regularizer by a sequence of regular functionals Ψ_ϵ using the Γ-convergence (we call MSAT, the Ambrosio and Tortorelli approximation of MS regularizer). The edge set K is represented by a smooth auxiliary function v. Shah [21] suggested a modified version of the AT approximation to the MS functional by replacing $|\nabla u|^2$ by $|\nabla u|$ (we call it MSTV). Furthermore, Bar et al [4] used the color versions of these functionals for color image deblurring-denoising by replacing the magnitude of the gradient

$|\nabla u|$ by the Frobenius norm of the matrix ∇u, $\|\nabla u\| = \sqrt{\sum_i [(u_x^i)^2 + (u_y^i)^2]}$ with $i \in \{r, g, b\}$ in the RGB color space, suggested by Brook et al [7]:

$$\Psi_\epsilon^{MSAT}(u,v) = \beta \int_\Omega v^2 \|\nabla u\|^2 dx + \alpha \int_\Omega \Big(\epsilon |\nabla v|^2 + \frac{(v-1)^2}{4\epsilon}\Big) dx,$$
$$\Psi_\epsilon^{MSTV}(u,v) = \beta \int_\Omega v^2 \|\nabla u\| dx + \alpha \int_\Omega \Big(\epsilon |\nabla v|^2 + \frac{(v-1)^2}{4\epsilon}\Big) dx$$

where $0 \leq v(x) \leq 1$ represents the edges: $v(x) \approx 0$ if $x \in K$ and $v(x) \approx 1$ otherwise, and $\alpha, \beta > 0$, $\epsilon \to 0$ are parameters. Note that, in both regularizers, the edge map v is common for the three channels and provides the necessary coupling between colors.

Nonlocal regularizer. Nonlocal methods in image processing have been explored in many papers because they are well adapted to texture denoising while the standard denoising models working with local image information seem to consider texture as noise, which results in losing details. Nonlocal methods are generalized from neighborhood filters and patch based methods. The idea of neighborhood filter is to restore a pixel by averaging the values of neighboring pixels with a similar color value. Buades et al. [8] generalized this idea by applying the patch-based method, and proposed the famous nonlocal-means (or NL-means) filter for denoising, given by $NLu(x) = \frac{1}{C(x)} \int_\Omega e^{-\frac{d_a(u(x),u(y))}{h^2}} u(y) dy$, where $u(y)$ is the color at y, $d_a(u(x),u(y)) = \int G_a(t) \|u(x+t) - u(y+t)\|^2 dt$ is the patch distance, G_a is the Gaussian kernel with standard deviation a determining the patch size, $C(x) = \int_\Omega e^{-\frac{d_a(u(x),u(y))}{h^2}} dy$ is a normalization factor, and h is the filtering parameter corresponding to the noise level (usually the standard deviation of the noise). The NL-means not only compares the color value at a single point but the geometrical configuration in a whole neighborhood (patch).

In the variational framework, Kindermann et al [13] formulated the neighborhood filters and NL-means filters as nonlocal regularizing functionals which generally are not convex. Then, Gilboa-Osher [10], [11] formalized the convex nonlocal functional inspired from graph theory, based on the gradient and divergence definitions on graphs in the context of machine learning. Let $u : \Omega \to \mathbb{R}$ be a function, and $w : \Omega \times \Omega \to \mathbb{R}$ be a nonnegative and symmetric weight function. The nonlocal gradient vector $\nabla_w u : \Omega \times \Omega \to \mathbb{R}$ is $(\nabla_w u)(x,y) := (u(y) - u(x))\sqrt{w(x,y)}$. Hence, the nonlocal divergence $\mathrm{div}_w \overrightarrow{v} : \Omega \to \mathbb{R}$ of the vector $\overrightarrow{v} : \Omega \times \Omega \to \mathbb{R}$ is defined as the adjoint of the nonlocal gradient, $(\mathrm{div}_w \overrightarrow{v})(x) := \int_\Omega (v(x,y) - v(y,x))\sqrt{w(x,y)} dy$, and the norm of the nonlocal gradient of u at $x \in \Omega$ is given by $|\nabla_w u|(x) = \sqrt{\int_\Omega (u(y) - u(x))^2 w(x,y) dy}$. Based on these nonlocal operators, they introduced nonlocal regularizing functionals of the general form $\Psi(u) = \int_\Omega \phi(|\nabla_w u|^2) dx$, where $s \mapsto \phi(s)$ is a positive function, convex in $\sqrt{s}$, and $\phi(0) = 0$. By taking $\phi(s) = \sqrt{s}$, they proposed the nonlocal TV regularizer (NL/TV) which corresponds in the local case to $\Psi^{TV}(u) = \int_\Omega |\nabla u| dx$. Inspired by these ideas, we propose in the next section

nonlocal versions of Ambrosio-Tortorelli and Shah approximations to the MS regularizer for color image restoration. This is also continuation or nonlocal extension of the work by Bar et al. [4], first to propose the use of local Mumford-Shah-like approximations to color image restoration. Part of this work is a generalization of [12].

3 Description of the Proposed Models

We propose the following nonlocal Mumford-Shah regularizers (NL/MS) by applying the nonlocal operators to the multichannel approximations of the MS regularizer

$$\Psi^{NL/MS}(u,v) = \beta \int_\Omega v^2 \phi(\|\nabla_w u\|^2) dx + \alpha \int_\Omega \Big(\epsilon |\nabla v|^2 + \frac{(v-1)^2}{4\epsilon}\Big) dx$$

where $u : \Omega \to \mathbb{R}^3$, $v : \Omega \to [0,1]$, $\phi(s) = s$ or $\phi(s) = \sqrt{s}$ correspond to the nonlocal versions of MSAT and MSTV regularizers, so called NL/MSAT and NL/MSTV, respectively. In addition, we apply these nonlocal MS regularizers to color image denoising, color image deblurring in the presence of Gaussian or impulse noise, color image inpainting, and moreover, to color image super-resolution, by incorporating proper fidelity terms. We define the weight function w using the noisy-blurry data f as $w(x,y) = e^{-\frac{d_a(f(x),f(y))}{h^2}}$, but we will see that this definition must be modified sometimes. Also, note that the nonlocal and nonconvex continuous models proposed in the following sections have not been analyzed theoretically; however, these formulations become well-defined in the discrete, finite differences case, but we prefer to present them in the continuous setting for simplicity.

3.1 Color Image Deblurring and Denoising

The degradation model for deblurring-denoising (or denoising) is given by $f_i = k * u_i + n_i$, with a (known) space-invariant blurring kernel k. First, in the case of Gaussian noise model, the L^2-fidelity term led by the maximum likelihood estimation is commonly used: $\Phi(f - k*u) = \int_\Omega \sum_i |f^i - k*u^i|^2 dx$. However, the quadratic data fidelity term considers the impulse noise, which might be caused by bit errors in transmissions or wrong pixels, as an outlier. So, for the impulse noise model, the L^1-fidelity term is more appropriate, due to its robustness of removing outlier effects [1], [17]; moreover, we consider the case of independent channels noise [4]: $\Phi(f - k*u) = \int_\Omega \sum_i |f^i - k*u^i| dx$. Thus, we design two types of total energies for color image deblurring-denoising, depending on the type of noise as follows:

$$\text{Gaussian noise:} \quad E^G(u,v) = \frac{1}{2} \int_\Omega \sum_i |f^i - k*u^i|^2 dx + \Psi^{NL/MSTV}(u,v) \quad (2)$$

$$\text{Impulse noise:} \quad E^{Im}(u,v) = \int_\Omega \sum_i |f^i - k*u^i| dx + \Psi^{NL/MSAT}(u,v). \quad (3)$$

Note that, for the impulse noise model, MSAT regularizer produces better results (especially in the presence of high density of noise), while for the Gaussian noise model, MSTV regularizer produces better results.

To extend the nonlocal methods to the impulse noise case, we need a preprocessing step for the weight function w since we cannot directly use the data f to compute w. In other words, in the presence of impulse noise, the noisy pixels tend to have larger weights than the other neighboring points, so it's likely to keep the noise value at such pixel. Thus, we propose a simple algorithm to obtain a preprocessed image g, which removes the impulse noise (outliers) as well as preserves the textures as much as we can. Basically, we use the median filter, well-known for removing impulse noise. However, for the deblurring-denoising model, if we apply one-step of the median filter, then the output may be too smoothed out. In order to preserve fine structures as well as to remove noise properly, we define a preprocessing method for the deblurring-denoising model inspired by the idea of Bregman iteration [6]. Thus, we propose the following algorithm to obtain a preprocessed image g that will be used only in the computation of the weight function w:

Initialize : $r_0^i = 0$, $g_0^i = 0$, $i = r, g, b$.
do (iterate $n = 0, 1, 2, \ldots$)
$g_{n+1} = median(f + r_n, [a\ a])$
$r_{n+1} = r_n + f - k * g_{n+1}$
while $\sum_i \|f^i - k * g_n^i\|_1 > \sum_i \|f^i - k * g_{n+1}^i\|_1$
[Optional] $g_m = median(g_m, [b\ b])$

where f is the given noisy-blurry data, and $median(f, [a\ a])$ is the median filter of size $a \times a$ with input f. The optional step is needed in the case when the final g_m still has some salt-and-pepper-like noise left. The preprocessed image g_m is a deblurred and denoised version of f; it will be used only in the computation of the weights w, while keeping f in the data fidelity term, thus artifacts are not introduced by the median filter. Note that for denoising only (no blurring), we apply the adaptive median filter or the median filter to the noisy image f, to produce a preprocessed image g.

3.2 Color Image Inpainting

Inpainting corresponds to the operation H of losing pixels from an image, i.e. the observed data f is given by $f = u$ on $\Omega - D$ with the region $D = D^0$ where the input data u has been damaged. Thus, we formulate the total energy functional for color image inpainting as

$$E^{Inp}(u, v) = \frac{1}{2} \int_{\Omega} \lambda_D(x) \sum_i |f^i - u^i|^2 dx + \Psi^{NL/MS}(u, v), \tag{4}$$

where $\lambda_D(x) = 0$ at $x \in D$ and $\lambda_D(x) > 0$ on $x \in \Omega - D$. In addition, we update the weights w only in the damaged region D^0 in every mth iteration for u using the patch distance: $d_a^R(u(x), u(y)) = \int_{\Omega - R} G_a(t) \|u(x + t) - u(y + t)\|^2 dt$, where

$R \subset D^0$ is an un-recovered region (still missing region). Therefore, the missing region D^0 is recovered by the following iterative algorithm, producing the un-recovered regions D^i, $i = 0, 1, 2, ...$, with $D^0 \supset D^1 \supset D^2 \supset \cdots$:

1. Compute weights w for $x \in \Omega$ s.t. $P(x) \bigcap (\Omega - D^0) \neq 0$ with $d_a^{D^0}(u^0(x), u^0(y))$, $u^0 = f$, and a patch $P(x)$ centered at x.
2. Iterate $n = 1, 2, ...$ to get a minimizer (u, v) starting with $u = u^0$:
   a. For fixed u, update v in Ω to get v^n.
   b. For fixed v, update u in Ω to get u^n with a recovered region $\Omega - D^n \supset \Omega - D^0$: at every mth iteration, update weights w only in $x \in D^0$ s.t. $P(x) \bigcap (\Omega - D^{n,m}) \neq 0$ with $d_a^{D^{n,m}}(u(x), u(y))$ where $D^{n,m}$ is an un-recovered region in D^0 until mth iteration with $D^{n,m} \supset D^{n,2m} \supset \cdots \supset D^{n,n} = D^n$.

3.3 Color Image Super-Resolution

Super-resolution of a single still image corresponds to the recovery of a high resolution image from a filtered and down-sampled image, i.e., the observed data f is given by $f^i = D_k(h * u^i)$, $i \in r, g, b$ where h is a low-pass filter, $D_k : \mathbb{R}^n \to \mathbb{R}^p$, $p = \frac{n}{k^2}$, is the down-sampling operator by a factor k along each axis. We want to recover a high resolution image $u \in (\mathbb{R}^n)^3$ by minimizing

$$E^{Sup}(u, v) = \frac{1}{2} \int_\Omega \sum_i |f^i - D_k(h * u^i)|^2 dx + \Psi^{NL/MS}(u, v). \tag{5}$$

In addition, we use a super-resolved image $g \in (\mathbb{R}^n)^3$ obtained by a bicubic interpolation of $f \in (\mathbb{R}^p)^3$ only for the computation of the weights w. We refer to [15,19] for prior relevant work.

3.4 Optimality Condition for (2)-(5)

Finally, minimizing the proposed functionals (2)-(5): E^G, E^{Im}, E^{Inp}, E^{Sup} in u and v, we obtain the Euler-Lagrange equations

$$\begin{aligned}
\frac{\partial E^{G,Im,Inp,Sup}}{\partial v} &= 2\beta v \phi(\|\nabla_w u\|^2) - 2\epsilon\alpha \triangle v + \alpha \left(\frac{v - 1}{2\epsilon} \right) = 0, \\
\frac{\partial E^G}{\partial u} &= \tilde{k} * (k * u - f) + L^{NL/MSTV} u = 0, \\
\frac{\partial E^{Im}}{\partial u} &= \tilde{k} * \text{sign}(k * u - f) + L^{NL/MSAT} u = 0, \\
\frac{\partial E^{Inp}}{\partial u} &= \lambda_D (u - f) + L^{NL/MS} u = 0, \\
\frac{\partial E^{Sup}}{\partial u} &= \tilde{h} * (D_k^T (D_k (h * u) - f)) + L^{NL/MS} u = 0,
\end{aligned}$$

where $\tilde{k}(x) = k(-x)$, $\tilde{h}(x) = h(-x)$, $D_k^T : (\mathbb{R}^p)^3 \to (\mathbb{R}^n)^3$ is the transpose of D_k i.e. the up-sampling operator, and

$$L^{NL/MS}u = -2\int_\Omega \Big\{(u(y)-u(x))w(x,y) \cdot \left[(v^2(y)\phi'(\|\nabla_w u\|^2(y)) + v^2(x)\phi'(\|\nabla_w u\|^2(x))\right]\Big\}dy.$$

To solve two Euler-Lagrange equations simultaneously, the alternate minimization approach is applied. Note that since the energy functionals are not convex in the joint variable (u, v), we may compute only a local minimizer. However, this is not a drawback in practice, since the initial guess for u in our algorithm is the data f (except for the super-resolution problem). Due to its simplicity, we use Gauss-Seidel scheme for v, and an explicit scheme for u using gradient descent method.

4 Experimental Results and Comparisons

The nonlocal MS regularizers proposed here, NL/MSTV and NL/MSAT, are tested on several color images corrupted by different blur kernels or different noise types, on color images with some missing parts, as well as on a sub-sampled color image. We compare them with their local versions. For comparisons with TV and NL/TV models of Rudin-Osher and Gilboa-Osher, we refer the reader to [12] for the case of gray-scale images.

First, we use noisy Lena images only corrupted by Gaussian noise or salt-and-pepper noise in Fig. 1. As expected, NL/MSTV and NL/MSAT perform better than MSTV and MSAT respectively in the sense that not only they preserve fine scales such as textures, but also in the case of NL/MSTV, the model does not produce any staircase effect (appeared in MSTV). For the restoration of the image (c) with salt-and-pepper noise, we apply one-step adaptive median filter with the maximum size 7×7 and then 5×5 median filter to the noisy image f, to produce a preprocessed image (PSNR=26.8145) only for the computation of w, and moreover the edges v detected concurrently with the restoration process are presented for the nonlocal methods.

Next, we recover a blurred image contaminated by Gaussian noise or random-valued impulse noise in Figures 2, 3, 5-7. First, we test the local and nonlocal MSTV on the Barbara image in Fig. 2 with Gaussian blur and noise, and then we test the local and nonlocal MSAT on the Lena images in Fig. 5 and the Girl images in Fig. 6 with different blur kernels and random-valued impulse noise with different noise levels. More precisely, in Fig. 3 in the presence of blur and Gaussian noise, NL/MSTV recovers well the fine scales such as textures leading to cleaner image and higher PSNR, while with MSTV, the textures are more smoothed out during the denoising process. In Fig. 5, we restore the Lena images blurred with motion blur and then contaminated by random-valued impulse noise with different noise densities $d = 0.2, 0.4, 0.5$ using MSAT and NL/MSAT. By using a preprocessed image for the weights, NL/MSAT provides

Fig. 1. Recovery of noisy image $f = u + n$ and PSNR values. Top row: (a) original, (b) noisy image with Gaussian noise with $\sigma_n = 0.02$, (c) noisy image with salt-and-pepper noise with noise density $d = 0.3$. Middle row: recovered images of (b) and edge set v using MSTV: $\beta = 0.17$, NL/MSTV: $\beta = 0.07$. Bottom row: recovered images of (c) and edge set v using MSAT: $\beta = 6$, NL/MSAT: $\beta = 1.8$.

better results visually and according to PSNR. Moreover, in Fig. 6, we test MSAT and NL/MSAT on the Girl images with either (b) high blur and low noise or (d) low blur and high noise. The restorations of (b) are shown in the first row in Fig. 7. Both local and nonlocal MSAT provide reasonable results, but NL/MSAT produces less ringing effects especially appeared on the cloth part. With the data (c), NL/MSAT gives cleaner result and higher PSNR while MSAT still has some noise, which are shown in the second row in Fig. 7.

Fig. 2. Left to right: original image, blurry image with Gaussian blur with $\sigma_b = 1$, noisy-blurry image corrupted by Gaussian noise with $\sigma_n = 0.004$

MSTV: 23.7266 NL/MSTV: 24.6396

Fig. 3. Recovery of the noisy-blurry image in Fig. 2 using (left) MSTV: $\beta = 0.04$, (right) NL/MSTV: $\beta = 0.012$

In Figures 8-9 we use the NL/MS regularizers to recover images with textures and large missing portions. In Fig. 8, we observe that both nonlocal regularizers recover the missing parts very well, and moreover NL/MSTV gives slightly better result than NL/MSAT according to PSNR even though they visually seem to produce very similar results. However, in Fig. 9 with a real image, we only present the result of NL/MSAT since it provides slightly better result than NL/MSTV (PSNR=34.2406), especially better recovering the part damaged by the circle.

In Fig. 4, we recover an image filtered with a low-pass filter and then sub-sampled. The nonlocal regularizers provide higher PSNRs and better visual qualities providing cleaner edges, while the local ones produce some artifacts especially on the edges. In addition, NL/MSTV gives the best result providing visually sharper and cleaner image, and highest PSNR.

Finally, we note that the parameters α, β and ϵ were selected manually to provide the best PSNR results. The smoothness parameter β increases with the noise level, while the other parameters α, ϵ are approximately fixed such as

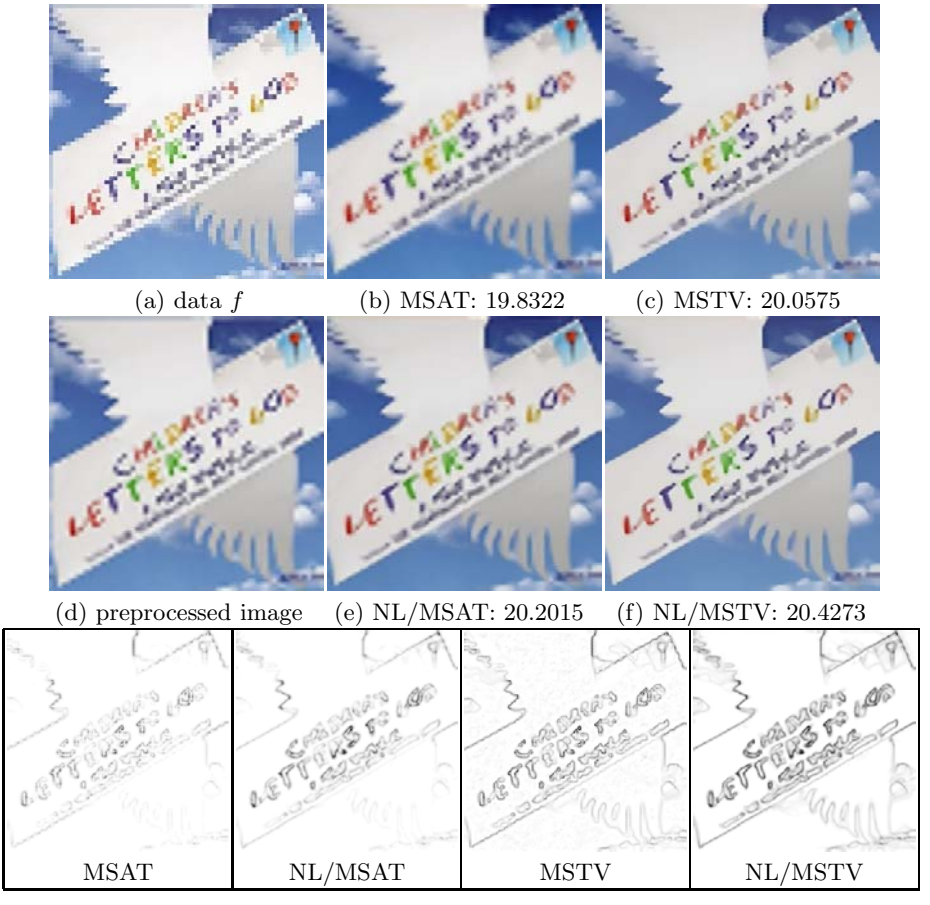

Fig. 4. Super-resolution of a low resolution image. (a) Data $f = D_k(h*u)$ of size 64×64 with uniform blur h of size 3×3 and sub-sampling factor $k = 4$, (d) a preprocessed image using bicubic interpolation (PSNR=18.0711), (b),(c),(e),(f): super-resolved images. Bottom: edge set v.

$\alpha = 0.1$, $\epsilon = 0.00000001$ for deblurring-denoising and inpainting model, and $\alpha = 0.1$, $\epsilon = 0.001$ for denoising and super-resolution (although in theory $\epsilon \to 0$, it is common in practice to work with a small fixed ϵ). For the weight function w, we use the search window $\Omega_w = \{y \in \Omega : |y - x| \leq r\}$ instead of Ω (semi-local) and the weight function w at $(x, y) \in \Omega \times \Omega$ depending on a function $g : \Omega \to \mathbb{R}^3$, $w(x, y) = exp\Big(-\frac{d_a(g(x),g(y))}{h^2}\Big)$. We use 11×11 search window with 5×5 patch for deblurring-denoising model (or denoising), and 21×21 search window with 9×9 patch for super-resolution, while larger search windows are needed for inpainting. For the computational time, it takes about 5 minutes for constructing the weight function of a 256×256 image with the 11×11 search window and 5×5 patch in MATLAB on a dual core laptop with 2GHz processor

Fig. 5. Recovery of blurry Lena image with several random-valued impulse noise levels, and PSNR values. Top row: original image, blurry image with motion blur kernel of length=10, oriented at angle $\theta = 25^\circ$ w.r.t. the horizon, a preprocessed image when $d = 0.2$ (PSNR=22.0317.) 1st column: (2nd to 4th row) noisy blurry data f with noise density $d = 0.2, 0.4, 0.5$. 2nd and 3rd columns: recovered images using (2nd) MSAT and (3rd) NL/MSAT. β (2nd to 4th row): 2, 4, 5 (MSAT), 0.3, 0.9, 1.2 (NL/MSAT).

(a) (b) (c) (d)

Fig. 6. Blurry image (a), noisy blurry image (b) with out-of-focus blur of radius 5 and radom-valued impulse noise of noise density $d = 0.2$. Blurry image (c), noisy blurry image (d) with out-of-focus blur of radius 3 and radom-valued impulse noise of noise density $d = 0.4$

Recovery of (b) using MSAT: 29.0399 vs NL/MSAT: 29.4242

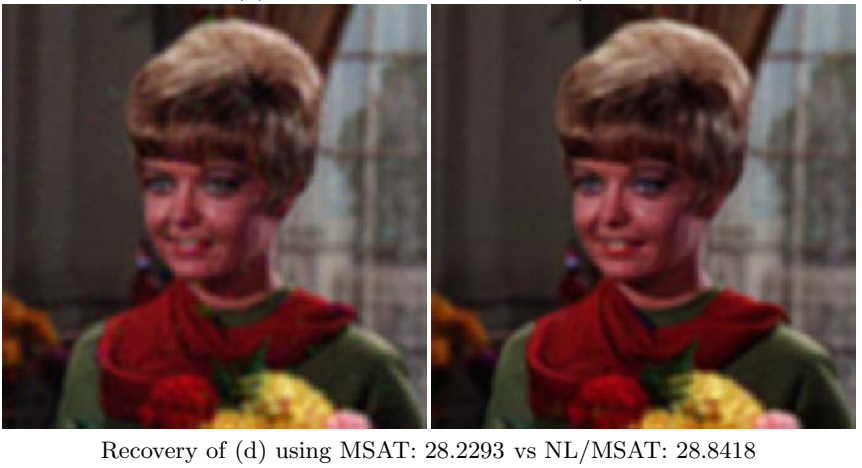

Recovery of (d) using MSAT: 28.2293 vs NL/MSAT: 28.8418

Fig. 7. Recovery of the noisy-blurry image (b) and (d) in Fig. 5 using MSAT (left), NL/MSAT (right) and PSNR values. Top: (MSAT) $\beta = 1$, (NL/MSAT) $\beta = 0.2$. Bottom: (MSAT) $\beta = 5$, (NL/MSAT) $\beta = 1.8$.

Fig. 8. Inpainting of 100×100 size image with 40×40 missing part. (left) data f, recovered using (middle) NL/MSAT: PSNR=35.6704, (right) NL/MSTV: PSNR=35.8024 (41×41 search window, 9×9 patch).

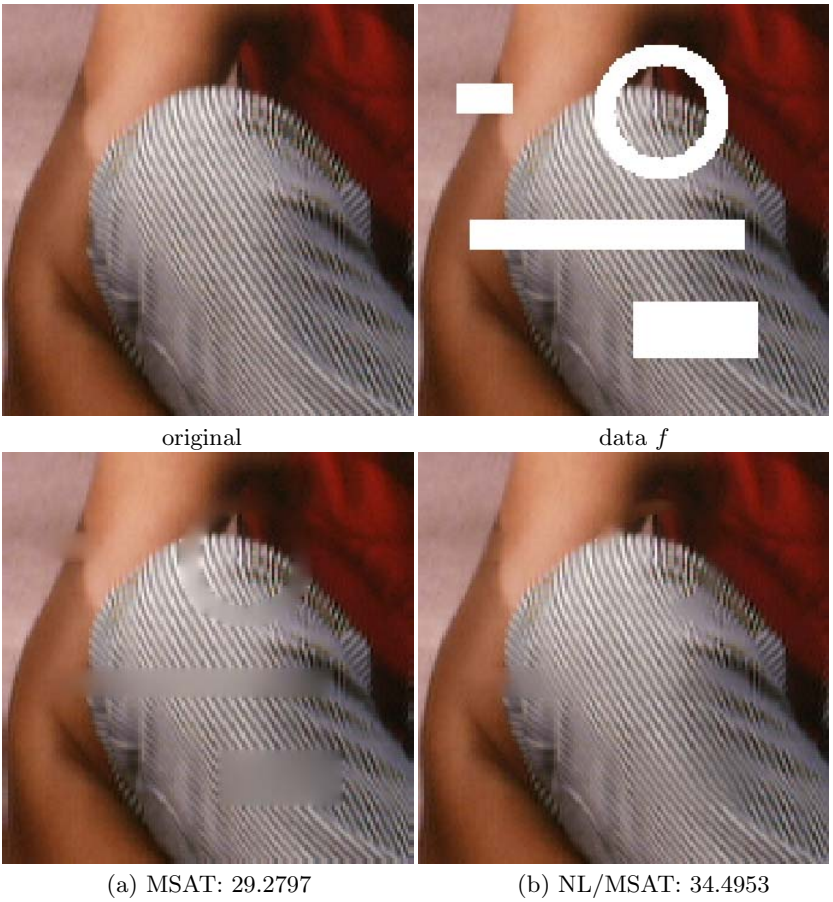

original data f

(a) MSAT: 29.2797 (b) NL/MSAT: 34.4953

Fig. 9. Inpainting of 150×150 size image. Top: (left) original, (right) data f. (a), (b): recovered images with (a) MSAT, (b) NL/MSAT (51×51 search window, 9×9 patch).

and 2GB memory. The minimization for the (local or nonlocal) MS regularizers in the deblurring-denoising model takes about 150 seconds for the computations of both u using an explicit scheme based on the gradient descent method and v using a semi-implicit scheme with the total iterations $5 \times (2 + 100)$ (without including the computation of the weight function $w(x, y)$). For inpainting model with 150×150 size image, it takes about 20 minutes with total iteration numbers $7 \times (2+100)$ since we update the weight function at every 50th iteration for u. For super-resolution, $10 \times (2 + 200)$ iteration numbers are needed for all regularizers.

5 Summary and Conclusions

The proposed nonlocal MS regularizers, NL/MSAT and NL/MSTV, outperform the local ones; in the image denoising or deblurring models in the presence of noise, NL/MSAT incorporating an efficient preprocessing step performs best for impulse noise, while NL/MSTV works best for Gaussian noise. Moreover, for super-resolution, NL/MSTV produces the best result with the sharpest and cleanest edges, while both NL/MSAT and NL/MSTV provide superior results in inpainting by recovering textures and large missing regions.

Acknowledgments. This work has been supported by the National Science Foundation Grants DMS- 0714945 and DMS-0312222.

References

1. Alliney, S.: Digital Filters as Absolute Norm Regularizers. IEEE TSP 40(6), 1548–1562 (1992)
2. Ambrosio, L., Tortorelli, V.M.: On the approximation of free discontinuity problems. BUMI 6-B, 105–123 (1992)
3. Bar, L., Sochen, N., Kiryati, N.: Image deblurring in the presence of impulsive noise. IJCV 70, 279–298 (2006)
4. Bar, L., Brook, A., Sochen, N., Kiryati, N.: Deblurring of Color Images Corrupted by Impulsive Noise. IEEE TIP 16(4), 1101–1111 (2007)
5. Blomgren, P., Chan, T.F.: Color TV: Total variation methods for restoration of vector-valued images. IEEE TIP 7(3), 304–309 (1998)
6. Bregman, L.M.: The relaxation method for finding common points of convex sets and its application to the solution of problems in convex programming. USSR Computational Mathematics and Mathematical Physics 7, 200–217 (1967)
7. Brook, A., Kimmel, R., Sochen, N.: Variational restoration and edge detection for color images. JMIV 18, 247–268 (2003)
8. Buades, A., Coll, B., Morel, J.M.: A review of image denoising algorithms, with a new one. SIAM MMS 4(2), 490–530 (2005)
9. Geman, D., Reynolds, G.: Constrained Restoration and the Recovery of Discontinuities. IEEE TPAMI 14(3), 367–383 (1992)
10. Gilboa, G., Osher, S.: Nonlocal linear image regularization and supervised segmentation. SIAM MMS 6(2), 595–630 (2007)
11. Gilboa, G., Osher, S.: Nonlocal operators with applications to image processing. SIAM MMS 7(3), 1005–1028 (2008)

12. Jung, M., Vese, L.A.: Nonlocal variational image deblurring models in the presence of Gaussian or impulse noise. LNCS, vol. 5567, pp. 402–413. Springer, Heidelberg (2009)
13. Kindermann, S., Osher, S., Jones, P.W.: Deblurring and denoising of images by nonlocal functionals. SIAM MMS 4(4), 1091–1115 (2005)
14. Lou, Y., Zhang, X., Osher, S., Bertozzi, A.: Image recovery via nonlocal operators. UCLA C.A.M. Report 08-35 (2008)
15. Malgouyres, F., Guichard, F.: Edge direction preserving image zooming: a mathematical and numerical analysis. SIAM NA 39(1), 1–37 (2001)
16. Mumford, D., Shah, J.: Optimal approximations by piecewise smooth functions and associated variational problems. CPAM 42, 577–685 (1989)
17. Nikolova, M.: Minimizers of cost-functions involving non-smooth data-fidelity terms. Application to the processing of outliers. SIAM NA 40(3), 965–994 (2002)
18. Peyré, G., Bougleux, S., Cohen, L.: Non-local regularization of inverse problems. In: Forsyth, D., Torr, P., Zisserman, A. (eds.) ECCV 2008, Part III. LNCS, vol. 5304, pp. 57–68. Springer, Heidelberg (2008)
19. Protter, M., Elad, M., Takeda, H., Milanfar, P.: Generalizing the Non-Local-Means to super-resolution reconstruction. IEEE TIP 18(1), 36–51 (2009)
20. Rudin, L., Osher, S.: Total variation based image restoration with free local constraints. IEEE ICIP 1, 31–35 (1994)
21. Shah, J.: A common framework for curve evolution, segmentation and anisotropic diffusion. In: IEEE CVPR, pp. 136–142 (1996)
22. Shen, J., Chan, T.F.: Variational image inpainting. CPAM 58(5), 579–619 (2005)